ISSN: 0974-5823 Vol. 6 No. 3 December, 2021

International Journal of Mechanical Engineering

Experimental Analysis for Fiber laser engraving process of AISI 202

Anita Pritam [1*], Rati Ranjan Dash [2], Ramesh Kumar Mallik [3]

[1] Ph.D. Research Scholar, [2] Professor, [3] Associate Professor

Mechanical Engineering, College of Engineering and Technology, Bhubaneswar, Odisha, India

Abstract: This paper investigates the effects of process parameters such as laser power, frequency, scan speed and fill spacing for laser engraving operation on AISI 202 material. The optimum parameter combination for minimizing the heat affected zone, and surface roughness are determined by using Taguchi's L16 orthogonal matrix with ANOVA analysis. A second order regression model was also developed to know the relationship between input parameters and output parameters. The outcomes of the regression model shows that the measured value from the model and experiments are so similar.

Keywords: laser engraving; HAZ width, Surface Roughness, Regression Model

1. Introduction

In recent years, the importance of microtechnology and non-traditional machining processes has skyrocketed [1]. Laser-assisted manufacturing is a conventional machining technique that removes material from the work surface using thermal energy. There have been numerous studies on laser-assisted material machining techniques. The majority of investigations look into the impact of process factors on surface roughness and lasers. However, there are just a few research on metal engraving and the HAZ width. Yasa et al. [2] investigated AISI 1045 steel selected laser erosion. They used the Nd.YAG laser sources to investigate the impact of operational factors on surface roughness in their research. The scan overlap, pulse overlap, and laser characteristics all have a substantial impact on the minimal surface roughness, according to their findings. Wendland et al. [3] used a laser to engrave deep into aluminium grade 5251 and stainless steel grade 316 for significant removal rates and surface modification under various process conditions. The impact of process variables (scan speed, frequency, power, overlapping, and scan strategy) on the surface roughness and depth of removed material was investigated by Campanelli et al. [4]. Pham et al. [5] conducted numerous experiments to determine the impact of laser milling operation variables (frequency, scan speed, pulse duration, and wavelength) on substance removal properties. Ceramic components were employed in the studies. Pham et al. [6] looked at how laser milling process factors affected the answers (surface finish, aspect ratio, accuracy, minimum feature size, etc.). They found that laser substrate contact and shorter pulse length affect accuracy and surface polish. Leone et al. [7] investigated the effect of process variables (multiple laser scanning, varying the pulse frequency, scanning speed, and scanning repetitions) on metals removal rates by engraving panels made of various types of wood with a Q-switched diode-pumped Nd:YAG green laser with a wavelength of 532 nm. The average power, pulse frequency, beam speed, and number of repetitions all have a significant impact on the etched depth, according to the researchers. With a Q-switched Nd:YAG laser, Chen et al. [8] employed the Taguchi technique to study the effect of five process factors (beam expansion ratio, focal length, average laser power, pulse repetition rate, and engraving speed) on the engraving line width. As a result, the brief literature review reveals that the majority of laser-assisted removal investigations focused on surface roughness utilising various approaches. However, it is well known that the machining procedure and process effectiveness are influenced by numerous process variables at different value, the kind of laser system, and the substance. The objective of this research is to furnish an idea on the engraving input and output results. The materials are mostly utilized in various engineering sectors like automotive, aerospace, various structural components, power plants etc. The detailed specifications are given in the following sections with its chemical compositions.

2. Experimental Details

The experiment was performed on AISI 202 by using laser fiber engraving machine to determine the best results of process responses such as HAZ Width and Surface Roughness (R_a). The most common material used, AISI 202 was taken for fiber laser engraving process. This material was chosen due to their day-to-day use in industrial field, house hold application, home decorative applications and other daily uses. AISI 202 is a steel alloy rich with chromium, Nickel and manganese as the alloying elements. AISI 202 is having high strength, toughness, hardness and good corrosion resistance mostly used in automotive applications, railroad coaches, kitchen utensils, indoor cladding etc. The job specimens were prepared having dimensions 25mm x 120 mm x1.5mm. Fig 1 represents the square engraved surface of AISI 202. The chemical composition of AISI is given on Table 1.

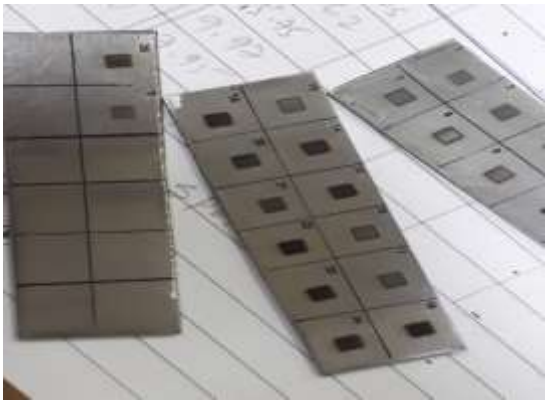

Fig 1 Engraved surface of AISI 202

Table 1 Chemical Composition of AISI 202 (weight %)

C	Mn	P	S	Si	Cr	Ni	N	Fe
0.15	7.8	0.06	0.015	0.6	17.61	5.1	0.15	balance

3. Experimental procedure and Process parameters

The engraving machining operation was conducted with the help of fiber laser engraving machine as shown in Fig 2, having wavelength of 1064 nm. The maximum power output of the laser machining set up is 100W. A computer (Fig 3) was connected to the laser set up having SIL software which was used to control the motion of laser beam and to adjust the input parameters for engraving machining. The job pieces were being constant over the fixed aluminium base plate in the machine set up. For preparing a 3x3 mm^2 square engraved parts for AISI 202, each machined parts were scanned by 30 times with parallel scan direction. All the experiments were performed at atmospheric conditions. To know the impact of input parameters on the engraving responses, initial tests were conducted before preparing the Taguchi's L_{16} test matrix. According to the initial tests, it was seen that power (P), frequency (F), fill spacing (FS) and scan speed (SS) were the four major parameters[9] which affect heat affected zone (HAZ) width and Surface Roughness (R_a) the most.

Fig 2 LASER Engraving machine

Fig 3 Full LASER engraving set up

During laser machining process, the area surrounded by the machined parts which were not melted but heated up to some extent and affect the microstructure of the material, are termed as heat affected zone which is to be minimized. By using a three-axis video inspection system with CNC control (Make: Baty, UK, Model: venture 3030 AB3-V-CNC), the HAZ width was measured by equation 1

$$HAZ\ width = \frac{HAZ\ circle\ diameter - Entry\ circle\ diameter}{2}\ mm \quad 1$$

A stylus profilometer Mitutoyo SJ 410 with a measurement of 1 mm long and cut length(c) and samples number (N) was measured to assess the surface roughness of the graved components. For each hole shape and square shape, six parallel measurements of the direction of the scan and six perpendicular measurements were selected and the final surface roughness was measured using an average of six measures (R_a in µm).

4. Design of experiment with experimental result Analysis for AISI 202

The experiments were performed on the basis of Taguchi L_{16} orthogonal array where 16 numbers of experimental runs were done for experimentation. The S/N ratio of all the responses at all level of variables were computed and the optimal combination of input parameters for all the four responses were calculated below the consecutive sections. Lastly the confirmation tests were performed to verify the best result obtained. The aim of this research work is to minimize the HAZ width and the Surface Roughness.

4.1 Statistical investigation

The process parameters chosen are Fill Spacing (FS), Power (P), Frequency (F) and Scan Sped (SS) with four different levels which are presented in Table 2.

Table 2 Process Parameters and their levels of AISI 202

Input Variables	Notations	Unit	Levels of factors			
			Level-1	Level-2	Level-3	Level-4
Fill spacing	FS	mm	0.01	0.015	0.02	0.025
Power	P	Watt	60	70	80	90
Frequency	F	KHz	20	25	30	35
Scan speed	SS	mm/s	100	200	300	400

Table 3 displays the output response and their corresponding S/N ratios of the laser engraving operation of AISI 202 material.

4.2 Parametric optimization of HAZ width

From Table 4, which is a response table of mean S/N ratio for heat affected zone, it is seen that scan speed is the most affecting parameters for HAZ followed by fill spacing and power and the least affecting parameter is the frequency which can also be verified by ANOVA table as given below in Table 5. Fig 4shows the optimum result for the response HAZ Width i.e., HAZ width is optimum at FS4-P2-F4-SS3. After obtaining the optimum value of process parameter (HAZ width), confirmation test was performed to examine the accuracy of the above result. By using optimal combination of process variables shown in Table 6, it is found that the upgraded value of S/N ratio from the initial to the optimal process variable is 5.63 dB.

Table 3 Experimental results with Taguchi L16 orthogonal array and their corresponding S/N ratio for AISI 202

Run No	Fill spacing (FS)	Power (P)	Frequency (F)	Scan speed (SS)	HAZ Width (mm)	S/N ratio	Surface Roughness (R_a)	S/N ratio
1	0.01	60	20	100	0.761	2.372	1.443	-3.185
2	0.01	70	25	200	0.624	4.096	1.342	-2.555
3	0.01	80	30	300	0.569	4.898	1.158	-1.274
4	0.01	90	35	400	0.533	5.465	1.776	-4.989
5	0.015	60	25	300	0.394	8.090	0.864	1.270
6	0.015	70	20	400	0.484	6.303	2.419	-7.673
7	0.015	80	35	100	0.738	2.639	2.779	-8.878
8	0.015	90	30	200	0.574	4.822	1.954	-5.818
9	0.02	60	30	400	0.547	5.240	1.504	-3.545
10	0.02	70	35	300	0.371	8.613	2.162	-6.697
11	0.02	80	20	200	0.366	8.730	2.220	-6.927
12	0.02	90	25	100	0.643	3.836	3.418	-10.675
13	0.025	60	35	200	0.378	8.450	3.545	-10.992
14	0.025	70	30	100	0.459	6.764	4.612	-13.278
15	0.025	80	25	400	0.469	6.577	1.058	-0.490
16	0.025	90	20	300	0.478	6.411	1.207	-1.634

Table 4 Response table of mean S/N ratio for surface HAZ Width for AISI 202

Notation	Input Variables	Mean S/N ratio					Rank
		Level 1	Level 2	Level 3	Level 4	Max-min	
FS	Fill spacing	4.208	5.463	6.605	7.050	2.843	2
P	Power	6.038	6.444	5.711	5.134	1.310	3
F	Frequency	5.954	5.650	5.431	6.292	0.861	4
SS	Scan speed	3.903	6.525	7.003	5.896	3.100	1
Total mean S/N ratio= 5.84dB							

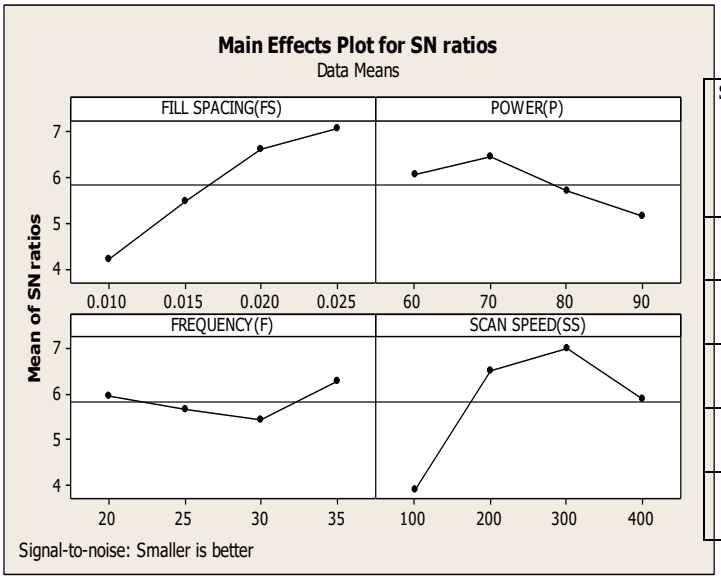

Fig 4 Main Effect plot for S/N ratio of HAZ Width for AISI 202

Table 5ANOVA for S/N ratio of the HAZ Width for AISI 202

Source	DF	Seq SS	Adj SS	Adj MS	f	p
FS	3	0.07190	0.07190	0.02397	1.37	0.401
P	3	0.01119	0.01119	0.00373	0.21	0.882
F	3	0.00245	0.00245	0.00082	0.05	0.984
SS	3	0.09084	0.09084	0.03028	1.73	0.331
Error	3	0.05243	0.05243	0.01748		
Total	15	0.22881				

Table 6 Result of confirmation of experiment for HAZ Width for AISI 202

	Initial process parameters	Optimal process parameters	
		prediction	experiment
level	FS P_3 F_4 SS_2		FS_4 P_2 F_4 SS_3
HAZ Width	0.684		0.358
S/N Ratio(dB)	3.29888	9.29413	8.92234
Improvement of S/N Ratio = 5.63dB			

4.3 Parametric optimization of Surface Roughness (R_a)

According to the mean S/N ratio response Table 7, Scan speed was found out to be the most influencing parameter for surface roughness for Al 6063 material whereas the power was discovered to be the least influential parameter for this engraving operation and that is also verified from ANOVA table as shown below, Table 8. From the primary plot of effect, the best results can be discovered by choosing the greatest values of S/N ratios which are displayed in Fig 5 below. It is seen that the best combination for minimizing the surface roughness is fill spacing at level-1, power at level-1, frequency at level-2 and scan speed at level-3 i.e., FS1-P1-F2-SS3.

Table 7 Response table of mean S/N ratio for surface roughness (R_a) for AISI 202

Symbol	Process parameters	Mean S/N ratio					Rank
		Level 1	Level 2	Level 3	Level 4	Max-min	
FS	Fill spacing	-3.001	-5.275	-6.961	-6.598	3.960	3
P	Power	-4.113	-7.551	-4.392	-5.779	3.437	4
F	Frequency	-4.855	-3.113	-5.979	-7.889	4.776	2
SS	Scan speed	-9.004	-6.573	-2.084	-4.174	6.920	1
Total mean S/N ratio= -5.46 dB							

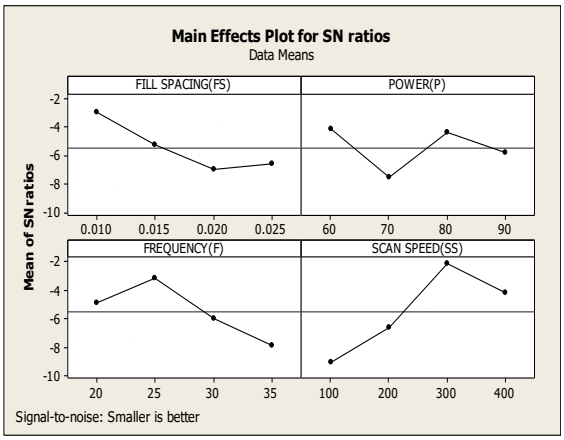

Fig 5 Main effect plot for S/N ratio for R_a for AISI 202

Table 8ANOVA for S/N ratio of R_a for AISI 202

Source	DF	Seq SS	Adj SS	Adj MS	f	p
FS	3	3.0590	3.0590	1.0197	1.08	0.476
P	3	1.7624	1.7624	0.5875	0.62	0.648
F	3	2.0834	2.0834	0.694	0.73	0.597
SS	3	6.7559	6.7559	2.2520	2.38	0.248
Error		2.8404	2.8404	0.9468		
Total	15	16.5011				

Table 9 Result of confirmation of experiment for surface roughness for AISI 202

	Initial process parameters	Optimal process parameters	
		prediction	Experiment
Level	FS_1-P_2-F_2-SS_3		FS_1-P_1-F_2-SS_3

Surface roughness	1.132		0.821
S/N Ratio(dB)	-1.07693	0.0130625	1.71314
Improvement of S/N Ratio = 0.64 dB			

Following the determination of the optimal machining parameter level, the prior investigation was confirmed. The test was thus carried out so that performance improvements may be anticipated and validated using the optimal combination of process parameters as indicated in Table 9. The enhancement in S/N ratio from the initial process parameter to the optimal process parameter will be calculated to be 0.64dB.

5. Development of mathematical model utilising Regression Analysis

Linear regression investigation was done from the experimental data to generate mathematical relationships between input variables and output responses.

5.1 Mathematical model for HAZ Width

The following equation was developed for HAZ width. The regression equation is:

HAZ Width = 6.23002 - 260.645*(FS) - 0.158672*(P) - 0.274647*(F) + 0.00933789*(SS) + 6585*(FS)*(FS) + 0.784887*(FS)*(P) - 0.0815157*(FS)*(F) + 0.0738519*(FS)*(SS) + 0.0035625*(P)*(P) + 0.008825*(P)*(F) - 0.000775*(P)*(SS) + 0.002675*(F)*(F) + 1.0875e-006*(SS)*(SS)

R-Sq = 98.40% R-Sq(adj) = 88.02%

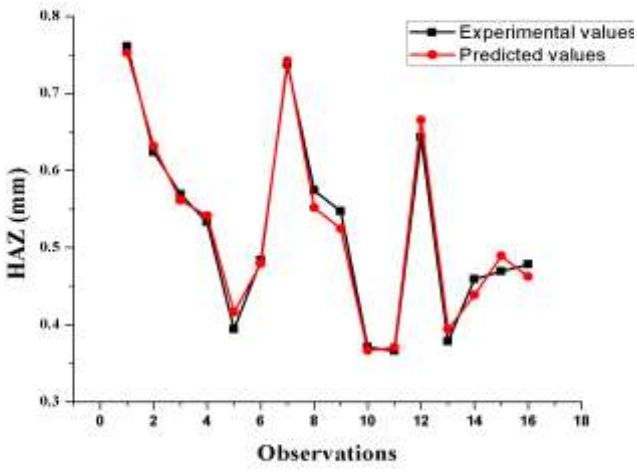

Fig 6 Experimental versus predicted values of HAZ Width for AISI 202

The comparison between experimental data with regression model value of HAZ Width value is shown in Fig 6. The forecasted values of HAZ in Regression models are nearly equal to experimental one. The maximum error between experimental and model values lies is considerably less. A good agreement has been established between predicted model and experimental value. Statistical analysis of variance ANOVA had been utilised for determining level of significance of the generated models. For laser engraving of AISI 202 alloy steel plate, this investigation shows the relative role of process variables in determining the response, i.e., heat affected zone. Table 10 represents the outcomes of analysis of variance for S/N ratio of HAZ width. Because the p value is below 0.05, the data follows a normal distribution, indicating that the mathematical proposed model by this formula is reasonable and acceptable. The graph between normal probability vs residuals of the Regression model is shown in Fig 7. The error terms are near to the straight path in the picture, implying that the errors are well evenly distributed and indicating that the components in the regression model are almost considerable.

Table 10 Analysis of Variance of HAZ model for AISI 202

Source	DF	Seq SS	Adj SS	Adj MS	f	p
Regression	13	0.225159	0.225159	0.0173199	9.47515	0.049398
Linear	04	0.118065	0.011406	0.0114055	6.23963	1.516008
Square	04	0.054937	0.010667	0.0106676	5.83588	1.75807
Interaction	05	0.052157	0.019968	0.0199693	10.92456	2.529708
Residual Error	2	0.003656	0.003656	0.0018279		
Total	15	0.228815				

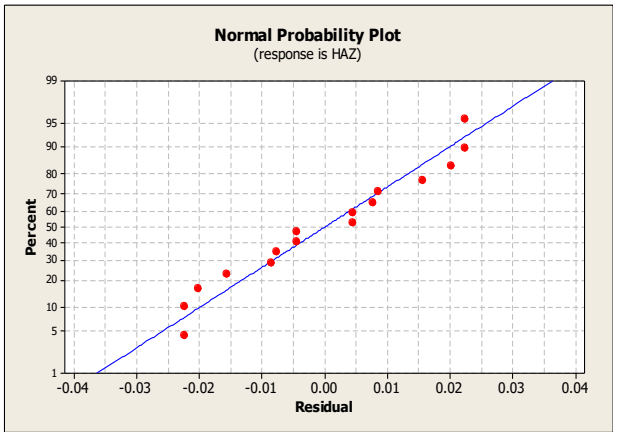

Fig 7 Normal Probability plot of residuals of HAZ Width for AISI 202

5.2 Mathematical Model of Surface Roughness

The regression equation is:

Surface Roughness (R_a) = 14.4321 - 580.894*(FS) + 0.89516*(P) - 1.6157*(F) + 0.0448774*(SS) + 18272.5*(FS)*(FS) - 9.76254*(FS)*(P) + 14.8267*(FS)*(F) - 0.790211*(FS)*(SS) - 0.0318594*(P)*(P) + 0.0370125*(P)*(F) - 0.0026525*(P)*(SS) + 0.0147125*(F)*(F) + 9.975e-006*(SS)*(SS)

R-Sq = 99.46% R-Sq(adj) = 95.93%

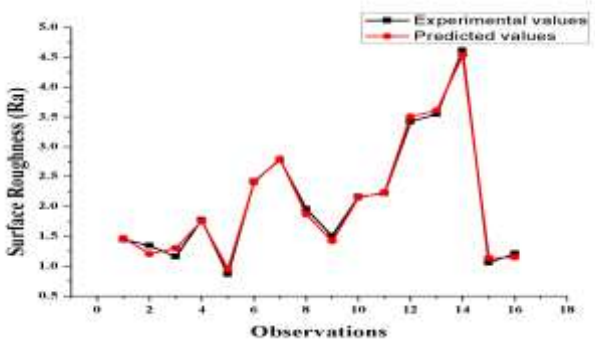

Fig 8 Experimental versus predicted values of surface roughness for AISI 202

The comparison between experimental data with the regression model value of Surface roughness value for AISI 202 is shown in Fig 8 and it is observed that the forecasted values of Surface roughness in Regression models are nearly same as experimental one.

Table 11 Analysis of Variance of R_a Regression Model for AISI 202

Source	DF	Seq SS	Adj SS	Adj MS	f	p
Regression	13	16.4116	16.4116	1.26243	28.1913	0.034757
Linear	04	9.6855	0.1868	0.18683	4.1722	1.698135
Square	04	1.8129	0.388	0.38809	8.6664	1.636208
Interaction	05	4.9131	2.4068	2.4068	53.7462	1.491785
Residual Error	02	0.0896	0.0896	0.04478		
Total	15	16.5011				

Table 11 represents the results of analysis of variance for the S/N ratio of the Surface Roughness for AISI 202. Because the p value is below 0.05, the data follows a normal distribution, indicating that the mathematical proposed model by this formula is reasonable and acceptable. The graph between normal probability vs residuals of the Regression model is represented by Fig 9. The error terms are near to the straight path in the picture, implying that the errors are well evenly distributed and indicating that the components in the regression model are almost considerable.

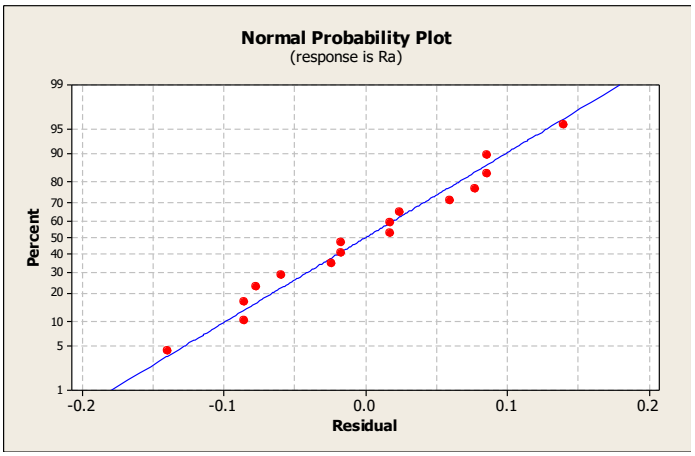

Fig 9 Normal Probability Plot of residuals of Surface Roughness for AISI 202

6. Result Discussion and Conclusion

The laser engraving operation on AISI 202 steel alloy was performed using fiber laser machining system. Based on Taguchi's orthogonal array and S/N survey, the optimal combination of all input variables was found out for individual output variables. Mathematical models had also been generated for individual responses utilizing regression analysis. The residuals in the normal probability graph are rather closer to the strait lines, implying that the variables indicated in the models are relevant. The use of this methodology improves the performance characteristics of the machining technique such as HAZ width and Surface roughness.

Reference

[1] Gillner, A.; Holtkamp, J.; Hartmann, C.; Olowinsky, A.; Gedicke, J.; Klages, K.; Bosse, L.; Bayer, A.: Laser applications in microtechnology. J. Mater. Process. Technol. 167, 494–498 (2005)

[2] Yasa, E.; Kruth, J.P.: Investigation of laser and parameters for selective laser erosion. Precision Eng. 34, 101–112 (2010)

[3] Wendland, J.P.; Harrison,M.; Henry, M.; Brownell, M.: Deep engraving of metals for the automotive sector using high average power diyod pumped solid state lasers. In: International congress on application of lasers and electro-optics, Miami, October (2005)

[4] Campanelli, S.L.; Ludovico, A.D.; Bonserio, C.; Cavalluzzi, P.; Cinquepalmi, M.: Experimental analysis of the laser milling process parameters. J. Mater. Process. Technol. 191, 220–223 (2007)

[5] Pham, D.T.; Dimov, S.S.; Petkov, P.V.: Laser milling of ceramic components. Int. J. Mach. Tools Manuf. 47, 618–626 (2007)

[6] Pham, D.T.; Dimov, S.S. Petkov, P.V.; Dobrev, T.: Laser milling for micro tooling. Laser metrology and machine performance. In: VIII Lamdamap Conference Proceedings, pp. 362–371 (2005)

[7] Leone, C.; Lopresto, V.; De Iorio, I.: Wood engraving by Q-switched diode-pumped frequency-doubled Nd:YAG green laser. Optics Lasers Eng. 47, 161–168 (2009)

[8] Chen, Y.H.; Tam, S.C.; Chen, W.L.; Zheng, H.Y.: Application of Taguchi method in the optimization of laser micro-engraving of photomasks. Int. J. Mater. Prod. Technol. 11, 333–344 (1996).

[9] A. Pritam, R.R. Dash and R.K. Mallik: Experimental investigation of fiber laser engraving operation on Al 6063, aluminium alloy, Elsevier, (article in press).